Journal of the Nigerian Association of Mathematical Physics
Volume **25 (November, 2013), pp 37 – 42**

Embedded atom method for face centered cubic metals: A Simple Algorithmic Approach

Matthew-Ojelabi F. and Ajibade I. I.

Department of Physics, Ekiti State University, PMB 5363, Ado Ekiti, Ekiti State. Nigeria

Abstract

An analytical expression derived for the embedding energy function $F(\rho)$ in an earlier work has been used to study more fcc monatomic metals. The parameters for the model were obtained from the available experimental physical quantities. Our physically well-motivated and transferrable $F(\rho)$ was able to reproduce the surface energies and other structural properties of nine fcc metals as established by the calculated results.

Keywords: Embedding energy method (EAM), Embedding energy function $F(\rho)$ and surface energies.

1.0 Introduction

The embedded atom method (EAM) which originated in [1] is still the most widely applied potential for pure metals and alloys. Our research group has already reported an embedding energy functional of form[2]

$$F(\rho) = AE_0\left(\frac{\rho}{\rho_0}\right)^{q_1} - AE_0\left(\frac{\rho}{\rho_0}\right)^{q_2}\ln\left(\frac{\rho}{\rho_0}\right) \tag{1.1}$$

where$A$, q_1 and q_2 are the adjustable parameters. The derivation of Eq.(1.1) was based on an overly simplified elastic energy expansion in Taylor's series with respect to small displacements and concurrently through the local density ρ leading to a second-order ordinary differential equation in $F(\rho)$. Eq.(1.1), though simple, contains the basic physical characteristics of the embedded atom method and provides another means of studying the functional dependence of EAM on the background density using certain empirical data. In the present work we report the results of the calculations of the surface energies performed with Eq.(1.1) for nine monatomic fcc metals.

The present work is organized as follows: Section 2 surveys briefly the physical theoretical requirements for the task. The calculation procedure is outlined in section 3 while the results, centred on nine face-centred-cubic (fcc) metals, are presented in section 4. Section 5 concludes the work.

1.0 Theory

EAM potential contains a many-body and a pairwise potential interaction terms designed to model the effective environment of an embedded atom. A heuristic derivation [1]using DFT led to

$$E_{tot} = \sum_i F_i\Big(\sum_{j\neq i}\rho_j^a\left(r_{ij}\right)\Big) + \frac{1}{2}\sum_{\substack{i,j\\ j\neq i}}\phi_{ij}\left(r_{ij}\right) \tag{2.1}$$

where

$$\rho = \sum_{j\neq i}\rho_j^a\left(r_{ij}\right) \tag{2.2}$$

Parameter ρ^a is the spherically averaged atomic density where $\rho_0 = \rho^a(r_0)$ represents the equilibrium value of the local density. The pair potential ϕ is an electrostatic two-body interaction. The host electron density ρ is assumed to be a linear superposition of contributions from individual atoms while $F(\rho)$ denotes the embedding energy functional. Eq.(2.1) is known for computational simplicity and it adequately caters for defects and other physical phenomena in solid or liquid state of metal. So far, EAM features the following three important functions: $F(\rho)$, $\rho(r)$ and $\phi(r)$.

The main tool for the present calculation is the embedding energy functional of Eq.(1.1) where

Corresponding author: ***Matthew-Ojelabi F.,*** E-mail: fadekematthew@yahoo.com, Tel.: +234 8030641917

$$F(\rho_0) = AE_0 \text{ and } F(0) = 0 \quad (2.3)$$

The vacancy formation energy is calculated from

$$E_{vac}^f = E_{tot}(vacanncy, N) - E_{tot}(perfect, N) \quad (2.4)$$

having defined E_{tot} in Eq.(2.1). For nearest-neighbour contribution in the fcc lattice, we have

$$\sum \rho(r_i) = 12\rho_0(r_0) \quad (2.5)$$

$$\sum \phi(r_{ij}) = 6\phi(r_0) \quad (2.6)$$

Let $\phi(r_0) = \phi_0$ so that Eq.(2.1) gives the following:

$$E_{tot}(perfect, N) = N\,F(12\rho_0) + \frac{1}{2}12N\phi_0 = N\,F(12\rho_0) + 6N\phi_0 \quad (2.7)$$

$$E_{tot}(vacancy, N) = (N-12)\,F(12\rho_0) + 12\,F(11\rho_0) + \frac{1}{2}(N-12)\phi_0 \quad (2.8)$$

Therefore from Eq.(2.4)

$$E_{vac}^f = -12\,F(12\rho_0) + 12\,F(11\rho_0) - 6\phi_0 \quad (2.9)$$

But the cohesive energy, by definition, is

$$E_{coh} = \frac{E_{tot}(perfect, N)}{N} = F(12\rho_0) + 6\phi_0 \quad (2.10)$$

leading to

$$6\phi_0 = E_{coh} - F(12\rho_0) \quad (2.11)$$

Thus,

$$E_{vac}^f = 12\,F(11\rho_0) - 11\,F(12\rho_0) - E_{coh} \quad (2.12)$$

Eq.(2.12) suggests that $E_{vac}^f \neq E_{coh}$ and for $E_{vac}^f < E_{coh}$ we must have

$$12\,F(11\rho_0) - 11\,F(12\rho_0) < 0 \quad (2.13)$$

or

$\frac{F(11\rho_0)}{11} < \frac{F(12\rho_0)}{12}$ which connotes $\frac{d^2F(\rho)}{d\rho^2} > 0$, a positive curvature.

2.0 Calculation Procedure: Application to the fcc lattice

The energies of monovacancy, divacancy, planar-surface formations etc. for the fcc metals are dominated by the contributions before relaxation. These energies are readily calculated from their analytic expressions if q_1, q_2 and A in Eq.(2.1) are known. The monovacancy formation energy, based on Eq.(2.4), is

$$E_{vac}^f = 12E_{11} - 12E_{12} \quad (3.1)$$

where

$$E_n = F\left(\frac{n}{12}\rho_0\right) + \frac{1}{2}\frac{n}{12}\phi_0 \quad (3.2)$$

$$E_{12} = E_0 = F(\rho_0) + \frac{1}{2}\phi_0 = -E_{coh} = \frac{E_{tot}}{N} \quad (3.3)$$

Therefore,

$$E_{vac}^f = 12F\left(\frac{11}{12}\rho_0\right) - E_0(1 + 11A) \quad (3.4)$$

The surface energies along the special directions are

$$\Gamma_{100} = \frac{2}{a^2}(E_8 - E_{12}) = \frac{2}{a^2}\left\{F\left(\frac{8}{12}\rho_0\right) - \frac{1}{3}E_0(1+2A)\right\} \quad (3.5)$$

$$\Gamma_{110} = \frac{\sqrt{2}}{a^2}(E_7 + E_{11} - 2E_{12}) = \frac{\sqrt{2}}{a^2}\left\{F\left(\frac{7}{12}\rho_0\right) + F\left(\frac{11}{12}\rho_0\right) - \frac{1}{2}E_0(1+3A)\right\} \quad (3.6)$$

$$\Gamma_{111} = \frac{4}{a^2\sqrt{3}}(E_9 - E_{12}) = \frac{4}{a^2\sqrt{3}}\left\{F\left(\frac{9}{12}\rho_0\right) - \frac{1}{4}E_0(1+3A)\right\} \quad (3.7)$$

where

$$F\left(\frac{7}{12}\rho_0\right) = AE_0\left(\frac{7}{12}\right)^{q_1} - AE_0\left(\frac{7}{12}\right)^{q_2}\ln\left(\frac{7}{12}\right) = F\left[\left(1 - \frac{5}{12}\right)\rho_0\right] \quad (3.8)$$

$$F\left(\frac{8}{12}\rho_0\right) = AE_0\left(\frac{8}{12}\right)^{q_1} - AE_0\left(\frac{8}{12}\right)^{q_2}\ln\left(\frac{8}{12}\right) = F\left[\left(1 - \frac{4}{12}\right)\rho_0\right] \quad (3.9)$$

$$F\left(\frac{9}{12}\rho_0\right) = AE_0\left(\frac{9}{12}\right)^{q_1} - AE_0\left(\frac{9}{12}\right)^{q_2}\ln\left(\frac{9}{12}\right) = F\left[\left(1 - \frac{3}{12}\right)\rho_0\right] \quad (3.10)$$

$$F\left(\frac{11}{12}\rho_0\right) = AE_0\left(\frac{11}{12}\right)^{q_1} - AE_0\left(\frac{11}{12}\right)^{q_2}\ln\left(\frac{11}{12}\right) = F\left[\left(1-\frac{1}{12}\right)\rho_0\right] \quad (3.11)$$

The following series expansions were employed in Eqs.(3.8 – 3.11):

$$\ln(1+x) = x - \frac{x^2}{2} + \frac{x^3}{3} - \cdots\cdots \quad (3.12)$$

and (binomial expansion)

$$(1+x)^n = 1 + \frac{nx}{1!} + \frac{n(n-1)x^2}{2!} + \cdots\cdots \quad (3.13)$$

Thus, we have

$$F\left[\left(1-\frac{n}{12}\right)\rho_0\right] = AE_0\left\{\begin{array}{l} 1+\frac{n}{12}\left[1+\frac{1}{2}\left(\frac{n}{12}\right)+\frac{1}{3}\left(\frac{n}{12}\right)^2+\frac{1}{4}\left(\frac{n}{12}\right)^3+\frac{1}{5}\left(\frac{n}{12}\right)^4+\cdots\cdots\right] \\ -\frac{n}{12}\left[1+\frac{1}{2}\left(\frac{n}{12}\right)+\frac{1}{3}\left(\frac{n}{12}\right)^2+\frac{1}{4}\left(\frac{n}{12}\right)^3+\frac{1}{5}\left(\frac{n}{12}\right)^4+\cdots\cdots\right]q_1 \\ +\frac{1}{2}\left(\frac{n}{12}\right)^2\left[1+\frac{1}{2}\left(\frac{n}{12}\right)+\frac{1}{3}\left(\frac{n}{12}\right)^2+\frac{1}{4}\left(\frac{n}{12}\right)^3+\frac{1}{5}\left(\frac{n}{12}\right)^4+\cdots\cdots\right]{q_1}^2 \\ -\frac{1}{3!}\left(\frac{n}{12}\right)^3\left[1+\frac{1}{2}\left(\frac{n}{12}\right)+\frac{1}{3}\left(\frac{n}{12}\right)^2+\frac{1}{4}\left(\frac{n}{12}\right)^3+\frac{1}{5}\left(\frac{n}{12}\right)^4+\cdots\cdots\right]{q_1}^3 \\ -\left(\frac{n}{12}\right)^2\left[1+\frac{1}{2}\left(\frac{n}{12}\right)+\frac{1}{3}\left(\frac{n}{12}\right)^2+\frac{1}{4}\left(\frac{n}{12}\right)^3+\frac{1}{5}\left(\frac{n}{12}\right)^4+\cdots\cdots\right]^2 q_2 \\ +\frac{1}{2}\left(\frac{n}{12}\right)^3\left[1+\frac{1}{2}\left(\frac{n}{12}\right)+\frac{1}{3}\left(\frac{n}{12}\right)^2+\frac{1}{4}\left(\frac{n}{12}\right)^3+\frac{1}{5}\left(\frac{n}{12}\right)^4+\cdots\cdots\right]^2{q_2}^2 \\ -\frac{1}{3!}\left(\frac{n}{12}\right)^4\left[1+\frac{1}{2}\left(\frac{n}{12}\right)+\frac{1}{3}\left(\frac{n}{12}\right)^2+\frac{1}{4}\left(\frac{n}{12}\right)^3+\frac{1}{5}\left(\frac{n}{12}\right)^4+\cdots\cdots\right]^2{q_2}^3 \end{array}\right\} \quad (3.14)$$

Table 1: Embedded Atom Method (EAM) (present work) and experimental parameters of selected nine*fcc* metals [3,4].

Metal	a_0 (Å)	E_{vac}^f(eV)	Fitting parameters		
			q_1	q_2	A
Ni	3.52	1.60	0.500	3.170	0.500
Cu	3.61	1.30	0.501	3.531	0.501
Ag	4.09	1.10	0.500	3.559	0.501
Pd	3.89	1.40	0.500	3.150	0.500
Rh	3.80	1.71	0.501	1.501	0.501
Ca	5.58	0.60	0.501	2.241	0.501
Sr	6.08	6.00	0.560	2.522	0.515
Ir	3.84	2.35	0.501	2.576	0.501
Th	5.08	2.00	0.501	2.146	0.501

3.0 Results and Discussion

We used Eq.(1.1) to calculate numerically the surface energies of each metal along the three different orientations (111), (110) and (100). The imputed experimental parameters were E_0, E_{vac}^f and lattice constant a. Parameters A, $q_1$and q_2 were adjusted to match the experimental value of E_{vac}^f (Eq.(3.4)). Our algorithm was based on a very simple procedure that

utilized about 1000 numerical grid pointswith spacing such that$\Delta A = \Delta q_1 = \Delta q_2 = 10^{-5}$. Thus, values of q_1, q_2 and A which fitted Eq.(3.4) perfectly were obtained for each metal.The results and other essential experimental parameters taken from Refs.[3, 4]were listed on Table1.Subsequently, the values of$A, q_1$and$q_2$were used in Eqs.(3.8 – 3.11) to calculate the low index surface energies. The results, compared to the first principle calculations [5,6,7], other EAM, MEAM [8,9,10,11] and experimental data [12] where available, were presented on Table 2.The embedding functional(Eq.(1.1))plotted using Nickel, Rhodium and Thorium data was displayed in Fig.1.

The fact that the equilibrium value of $F(\rho)$ was not noticeable at $\rho/\rho_0 = 1$ in Fig.1 as it should was attributed to the uncertainties in the experimental values of the cohesive energy.

Table 2: Unrelaxed surface energies (ergs/cm^2) of nine fcc metals compared with first principle, EAM, MEAM calculations and theexperimental values of the average surface energies.

Surface energies in ergs/cm^2										
Metal	Crystal Face (hkl)	EAM Present Work	First principle calculations			EAM		MEAM		Exp. (Ave.)
			A	B	C	D	E	F	G	
Ni	(100)	2622			2426	1580	1654	2435	1304	
	(110)	3999			2368	1730	1786	2384	1417	
	(111)	1876	2630		2011	1450	1540	2036	1170	2450
Cu	(100)	2088	2090		2166	1280	1260	1651	1006	
	(110)	3182	2310		2237	1400	1361	1642	1106	
	(111)	1477	1960		1952	1170	1180	1409	939	1830
Ag	(100)	1380	1200	1210	1200	705	821	1271	752	
	(110)	2104	1290	1266	1238	770	883	1222	833	
	(111)	976	1120	1210	1172	625	765	1089	713	1250
Pd	(100)	1873	1900	1860	2326	1370	1157	1659	1018	
	(110)	2856		1970	2225	1490	1240	1470	1119	
	(111)	1350	1880	1640	1920	1220	1074	1381	926	2050
Rh	(100)	1972	2900	2810	2799			2902	2137	
	(110)	3264		2880	2899			2921	2272	
	(111)	1479	2780	2530	2472			2598	1834	2700
Ca	(100)	359			542					
	(110)	564			582					
	(111)	263	352		567					450
Sr	(100)	310			408					
	(110)	496			432					
	(111)	225	287		428					410
Ir	(100)	3073			3722			2907	2569	
	(110)	4760			3606			3058	2664	
	(111)	2231			2971			2835	2038	3000
Th	(100)	1426			1468					
	(110)	2252			1450					
	(111)	1046			1476					1500

A: First principle calculations [5]
B: First principle calculations [6]
C: First principle calculations [7]
D: EAM calculations [8]
E: EAM calculations [9]
F: MEAM calculations [10]
G: MEAM calculations [11]

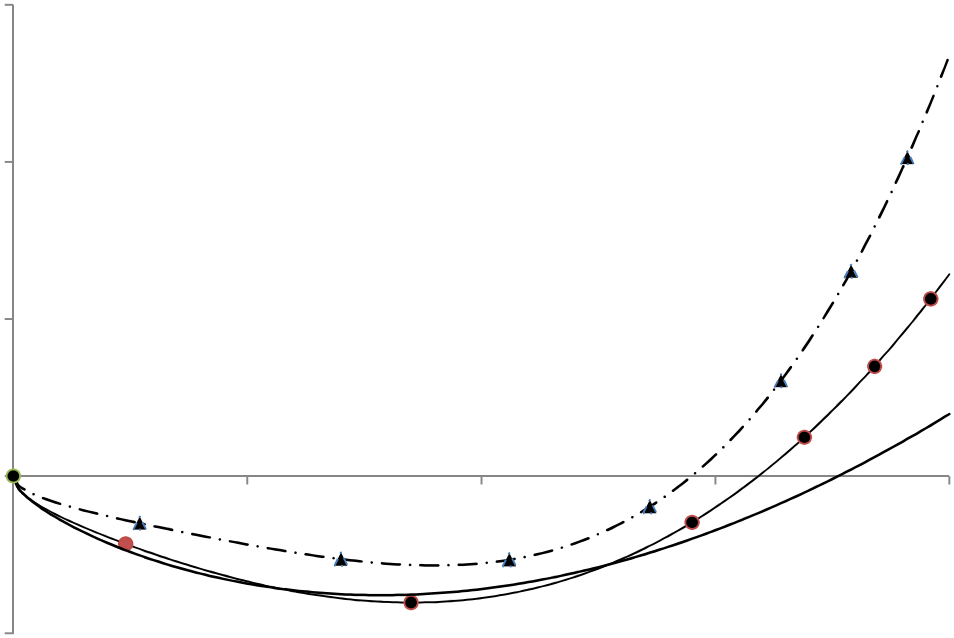

Figure 4.2: Embedding energy functional of present work: triangle (Nickel), bullet (Thorium), full-line(Rhodium).

4.0 Conclusion

The purpose of the present work was to capture the essence of EAM and by extension MEAM by taking into consideration the physical interpretation of each term involved in the elastic energy of a metal. Hence, we developed an analytic model for theembedding energy functional which reproduced very well some important features of the metals. The experimental inputs of our modelwere very few and thus gave it an edge over other EAM or MEAM models; these were the lattice constant, cohesive energy and the vacancy formation energy.

Our results for the nine fcc metals compared favourably with the available experimental and other theoretical data besides revealing that the first derivative rather than the second derivative of the embedding energy function dominated the values recorded for the embedding energy function. On the other hand, the curvature of the embedding energy function accounted for the many-body aspect of EAM or MEAM.

It should be stated that our calculation did not make use of the explicit form of the inter-atomic potential, instead $\phi_0$was subsumed into A. This is to say that our model is not constrained in any way by the specific form of the two-body potential. Whatever the form of $\phi(r_{ij})$, one can always find a means of incorporating it,together with other correlation effects, into the calculation for better results.

To appreciate the genuineness of our model (Eq.(1.1)), we have already extended our calculations to several bcc metals and the agreement with experiments was generally good. For further work, we are considering an extension to hcp metals and the inclusion of a background atomic density which is angular and reference-state dependent (MEAM).

References

[1] M. S. Daw,M. I. Baskes,Phys. Rev. B 29, 12 (1984) 6443-6453.

[2] F. Matthew-Ojelabi, J. O. A. Idiodi, I. I. Ajibade and O. Enoch, J. Nig. Ass. Math. Phys. (NAMP), 22 (2012) 35-42.

[3] C. Kittel, Introduction to Solid State Physics,Fifth ed., Wiley Eastern Limited, India (1985) 31-74.

[4] W. R. Tyson and W. A. Miller, Surf. Sci. 62 (1977) 267.

[5] H. L. Skriver and N. M. Rosengaard, Phys. Rev. B, 46, 11 (1988) 7157-7168.